TADEUSZ KORONOWICZ, Prof.,D.Sc.
TERESA TUSZKOWSKA, D.Sc.
TOMASZ WACŁAWCZYK, M.Sc.
Institute of Fluid Flow Machinery, Gdańsk
Polish Academy of Sciences

A computer method for prediction of the velocity field behind a full-scale ship hull

SUMMARY

One of the most important problems in the ship propulsion prognosing is determination of the full--scale velocity field within the propeller operation area behind the ship hull. Numerical calculation results of such velocity field, obtained by means of the own computer software PANSHIP-2 (the „numerical model basin") are presented in this paper.

Selected examples illustrate the influence of propeller operation on the effective field. Also, the scale effect of the nominal flow field is discussed.

INTRODUCTION

On the contemporary ships the criterion of the maximum pressure pulsation on the hull and the maximum bearing force criterion predominate over the demand of the maximum propulsion efficiency. In such cases it is necessary to know the velocity field behind the full--scale ship hull.

The present state of the *numerical model basin* development does not provide fully reliable results regarding the velocity field behind the hull. Therefore none of the experienced screw-propeller designers would be ready to base his propulsion prognosis only on results obtained by using a *numerical model basin* software. However, making an assumption that such calcultation is able provide reliable data about differences between the velocity field around the model (model's wake) and that around the full-scale ship with working propeller (effective wake), one can propose a method for predicting the velocity field behind the full-scale ship.

It consists in :

- calculation of differences between the velocity field for the model without working propeller and that for the full-scale ship with working propeller
- adding the differences to the nominal velocity field measured on the model.

The so obtained velocity field makes it possible to more correctly design the propeller for a real ship (the radial distribution of wake can be adjusted to the effective velocity field), and first of all it makes performing an appropriate analysis of the real propeller operation in the effective velocity field, possible.

An effectiveness condition for the proposed method is having at disposal a computer program suitable for appropriate taking into account the scale effect within the boundary layer, as well as accounting for the screw-propeller operation influence on the flow around the aft part of the hull and on a modification of the boundary layer over that area.

In this paper calculation results are presented which take into account both influences regarding the velocity field for three ship hull forms as follows :

$\Rightarrow$ a Wigley's hull of the block coefficient $C_B = 0.44$
$\Rightarrow$ a ship hull of Series 60 of $C_B = 0.60$
$\Rightarrow$ a modern containership hull of $C_B = 0.65$.

The presented material is hoped to be a suitable basis for broader discussion about prediction of the velocity field behind the full-scale ship hull.

THE COMPUTER MODEL BASIN SOFTWARE – PANSHIP-2

The computer model basin software PANSHIP-2 owned by the authors was put into operation eight years ago. It is under continuous refinement and updating with new calculation possibilities [2 , 4]. The basic assumptions for the calculation algorithm of the software in question (consisting of several independent programs) are the following:

The method of successive approximations is used to reach a solution :

1. 1st step - calculation of the velocity and pressure fields around a double hull deep-immersed in the ideal fluid, moving with a constant speed

2. Next, on the basis of the pressure field over the double-hull division area (Bernoulli wave) the secondary wave system around the hull is calculated, and the velocity and pressure fields on the hull are modified
3. In this step the velocity field within the boundary layer on the hull is calculated (the calculations are performed along the stream lines, and 1st approximation is made on the basis of integral equations of the boundary layer, whereas the next ones – of RANS equations), then the hull form is modified in accordance with the boundary thickness
4. The calculations are repeated for the modified hull form until an acceptable consistence of the calculation results obtained in successive calculation steps, is reached
5. In this step the nominal wake is calculated within the propeller operation area (the calculations are carried out on the basis of RANS equations for a space grid formed in the aft part of the hull).

After that phase of calculations the needed data regarding the **nominal velocity field** are obtained. That field can be used for preliminary design calculations of a propeller (however, model test results are more appropriate for that aim). The preliminary propeller design makes it possible to continue calculations already for the working propeller. In the successive steps the above presented calculations are continued, during which, however, new data regarding the propeller--induced velocity field on the hull, are added (they are taken into account in the boundary conditions) :

6. The hydrodynamic characteristics of the propeller in the nominal velocity field as well as the propeller-induced velocities in control points on the hull, are calculated
7. The calculations are repeated (as in p.4.) for new boundary conditions on the hull
8. The effective wake, new propeller performance parameter values and new propeller-induced velocities in control points on the hull, are calculated
9. The calculations specified in p. 7. and p. 8. are repeated until an acceptable consistence of the calculation results obtained in successive iteration steps is reached.

The second phase of the calculations is completed when acceptable differences of the calculation results obtained in the successive calculation steps is reached (in practice two steps of iteration are sufficient). A final calculation result is the **calculated effective wake**.

A comparative analysis of the obtained results and model test results shows their moderate consistence, however generally, the calculations performed with the use of PANSHIP-2 computer software correctly represent changes of the velocity field along with changes of hull form, of main dimensions and speed of a ship. Hence, in accordance with the presented method of the determination of the effective velocity field for a real ship, the PANSHIP-2 computer software can play an important role in the design process of screw propellers. Further work aimed at refinement of the computation algorithms of that software is underway.

CALCULATION RESULTS FOR THE „WIGLEY'S " HULL

The Wigley's hull form, familiar for the specialists in ship hydromechanics, can be entirely described by means of a simple analytical function. Its frame sections and waterlines are described by 2nd order parabolic functions. Such regular hull form is very suitable for testing computer-aided calculations of different kind. Panelization of the hull is easy, and its simple stern form facilitates shaping the behind-the-hull stream. Such form is excellent for testing the scale effect due to that stream.

In Fig.1 and 2 isotachs of the axial component of the nominal velocity field behind the hull, obtained from calculations performed for the ship of L = 200 m and its model of L = 2.5 m, at the Froude number Fn = 0. 2323, are presented.Images of the fields highly differ from each other. In which way the velocity fields are changing it can be better observed when analyzing the curves given in Fig.3. in the form of $V_x / V_s(\Phi)$, for r/R = const (where the reference field is that for 2.5 m model), as well as the diagram shown in Fig.4 where the flow-rate average of the axial velocity component within the propeller disc, is presented.

As the relationship between the boundary layer thickness and Reynold's number values is known, such result is not surprising, however it reveals quantitatively the scale-effect influence on the velocity field used for all calculations associated with ship screw propeller operation. The changes are very distinct both regarding the field itself and the average values. For the two remaining components of the field the changes are also significantly different; it can be observed in Fig.5 for the tangential component V_t / V_s, and in Fig.6 for the radial component V_r / V_s. The largest changes are located around the plane of symmetry of the hull, which is understandable in the case of single-propeller ships.

The calculation results obtained from the „computer model basin" also confirm the very strong influence of the scale effect on the effective velocity field. In Fig.7 the differences between the nominal velocity field and that effective for the 2.5 m model, and in Fig.8 - for

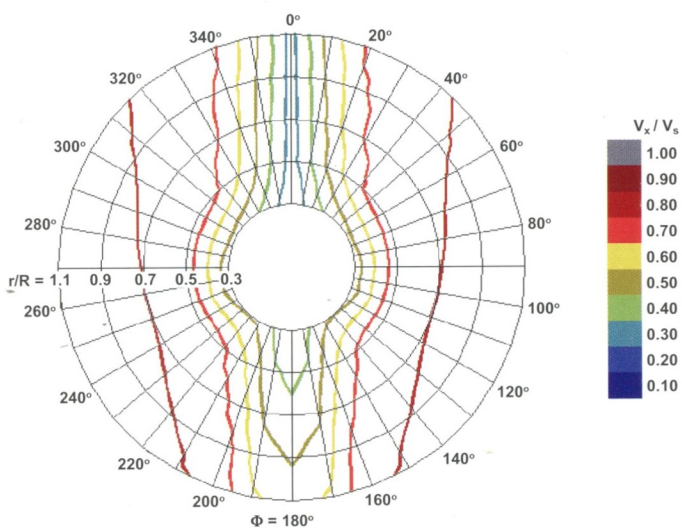

Fig.1. Isotachs of the axial component of the nominal velocity field behind the hull, obtained from calculations performed for 2.5 m model at V = 1.2 m/s (Fn = 0. 2323)

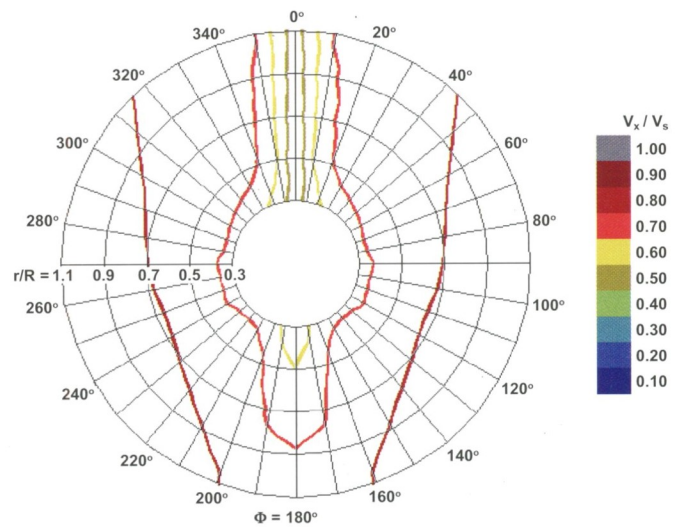

Fig.2. Isotachs of the axial component of the nominal velocity field behind the hull, obtained from calculations performed for 200 m ship, at V = 10.73 m/s (Fn = 0. 2323)

the 200 m ship, are presented. Comparing the figures one can firmly observe the greater influence of the propeller operation in the case of the 2.5 m model.

The above given comments clearly indicate that it is necessary, for the ship model testing centres, to have at their disposal a „computer model basin" for analytical determination of both the scale effect and the propeller influence on the velocity field within the propeller working disc.

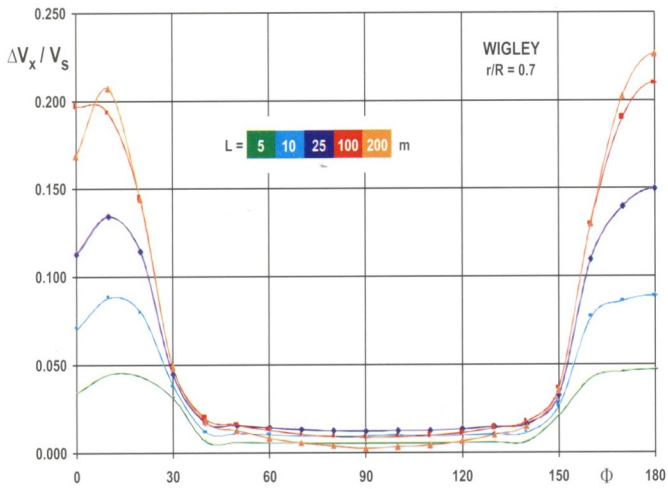

Fig.3. Nominal and effective wake fraction, $V_x/V_s(\Phi)$, at r/R = 0.7, for 2.5 m Wigley's ship model and the ship hulls of different length

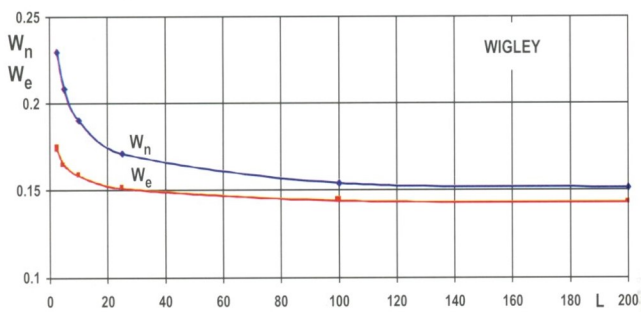

Fig.4. The flow-rate average of the axial velocity component within the propeller disc, in function of the ship length L, for Wigley's hull form

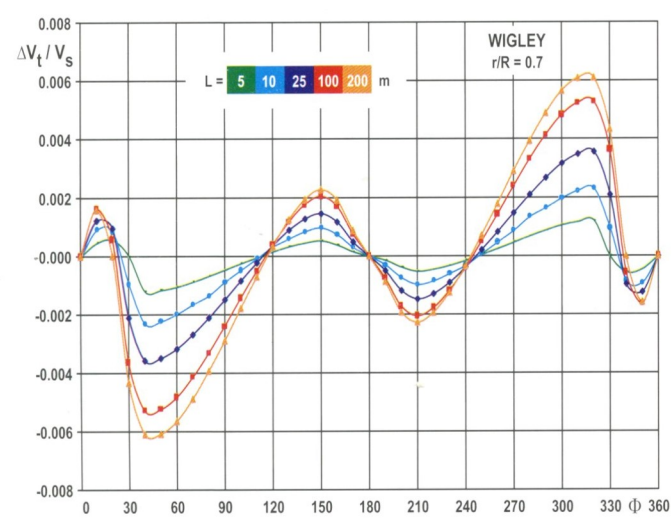

Fig.5. Differences between the tangential component of the nominal velocity field, $V_t/V_s(\Phi)$, at r/R = 0.7, for 2.5 m Wigley's ship model and the ship hulls of different length

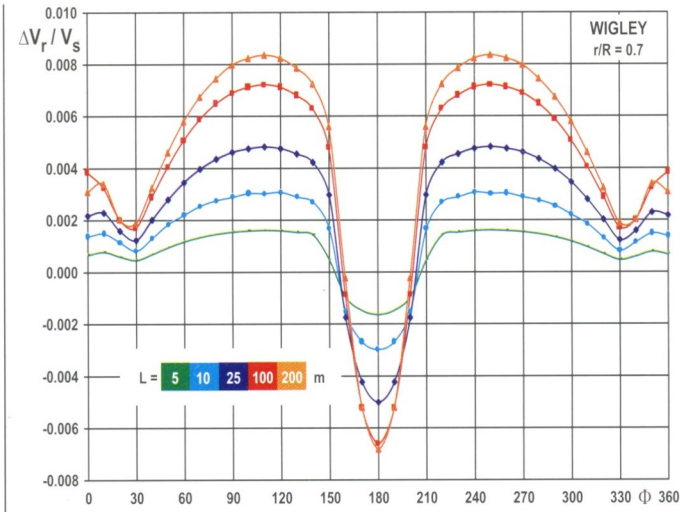

Fig.6. Differences between the radial component of the nominal velocity field, $V_r/V_s(\Phi)$, at r/R = 0.7, for 2.5 m Wigley's ship model and the ship hulls of different length

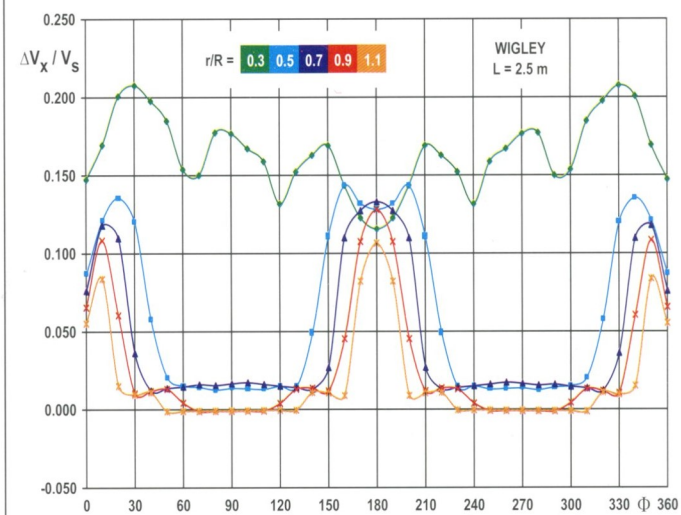

Fig.7. Differences between the axial components of the nominal velocity field and the effective one, $V_x/V_s(\Phi)$, at different r/R values, for 2.5 m Wigley's ship model

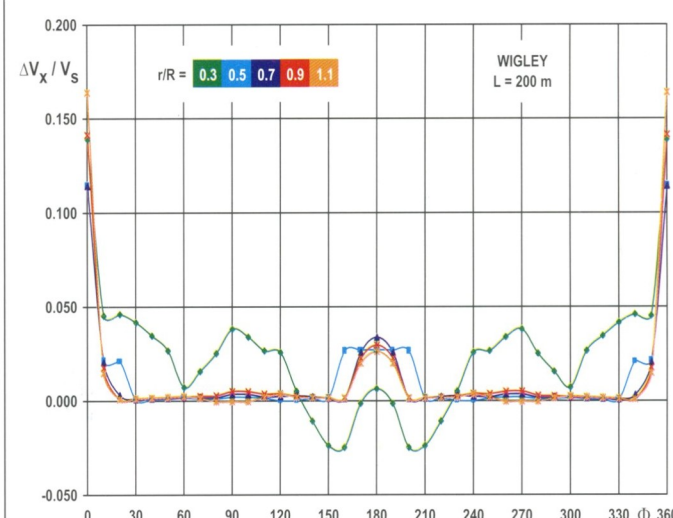

Fig.8. Differences between the axial components of the nominal velocity field and the effective one, $V_x/V_s(\Phi)$, at different r/R values, for 200 m Wigley's ship

CALCULATION RESULTS FOR THE HULL OF S-60 SERIES

For the hull of S-60 series, of $C_B = 0.6$, the data of its velocity field were available from relevant publications. The axial component of the velocity field, given in Fig.9, was used for the presented calculations. A representation of the velocity field obtained from the calculations, is shown in Fig.10. The differences between them are noticeable. Fig.11 presents differences between components of the effective velocity field for the ship of $L_{bp} = 200$ m and the nominal field for the model of $L_{bp} = 4$ m. The differences obtained from the calculations take significant values.

The axial component of the effective velocity field for the 200 m ship, obtained after the modification of the model's velocity field (by using the differences shown in Fig.11) is presented in Fig.12. And, Fig.13 shows the same component of the effective velocity field obtained from the calculations. The differences are distinct because they also account for the changes between the fields shown in Fig.9 and 10.

The changes in the velocity field result in the changes of the average values of the field. For instance, the radial distributions, presented in Fig.14, of the average value of the axial component of the field (wake fraction), for the nominal velocity field of the model and the ship, as well as for the effective field of the ship, indicate that the influence of the scale effect and of propeller operation on the course of these distributions is significant.

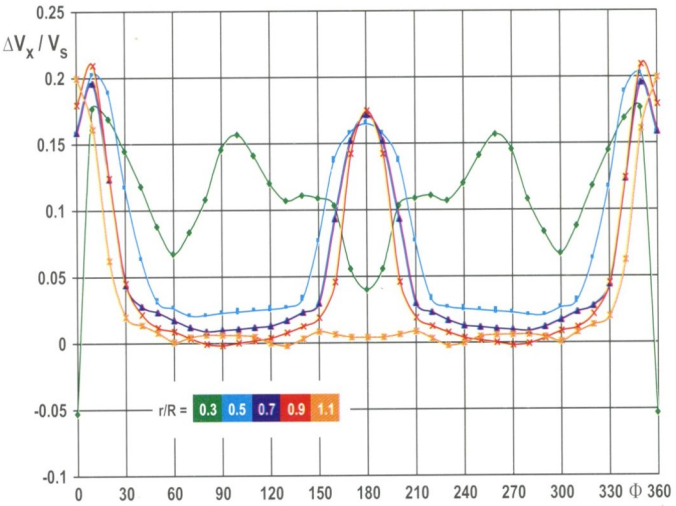

Fig.11. Differences, at different r/R values, between the axial component of the effective velocity field, V_x/V_s (Φ), for 200 m S-60 ship, and the axial component of the nominal velocity field for 4 m S-60 ship model

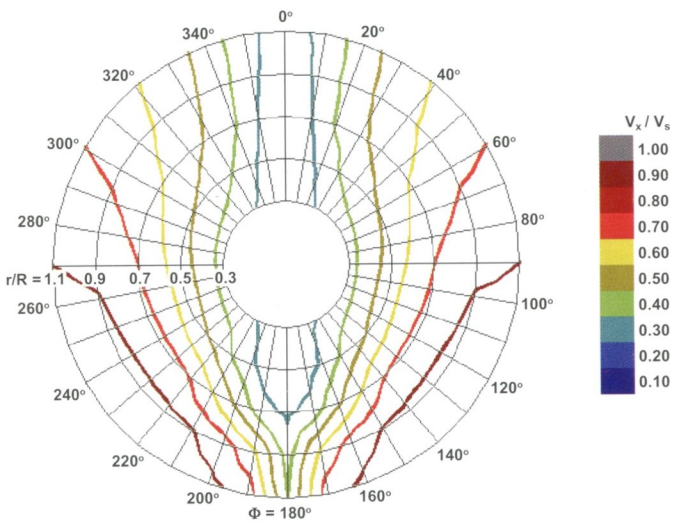

Fig.9. The axial component of the velocity field, obtained from the tests of 4 m S-60 ship model at V = 1.2 m/s

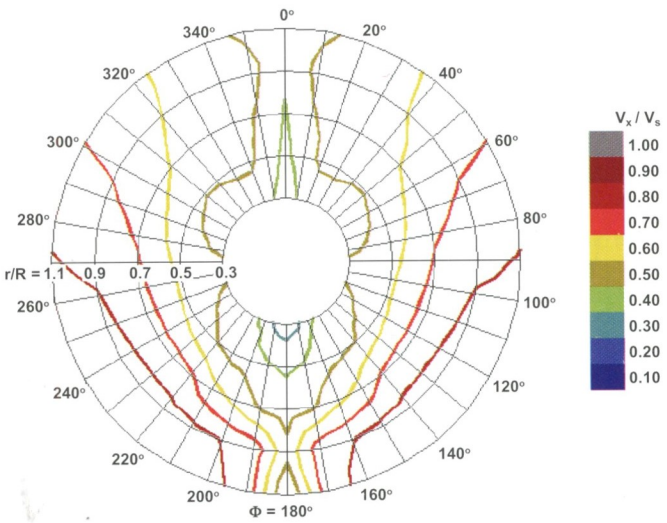

Fig.12. The axial component of the velocity field, for 200 m S-60 ship, obtained from the tests of its 4 m model, at V = 1.2 m/s, modified with the use of the differences V_x/V_s (Φ) obtained from the calculations

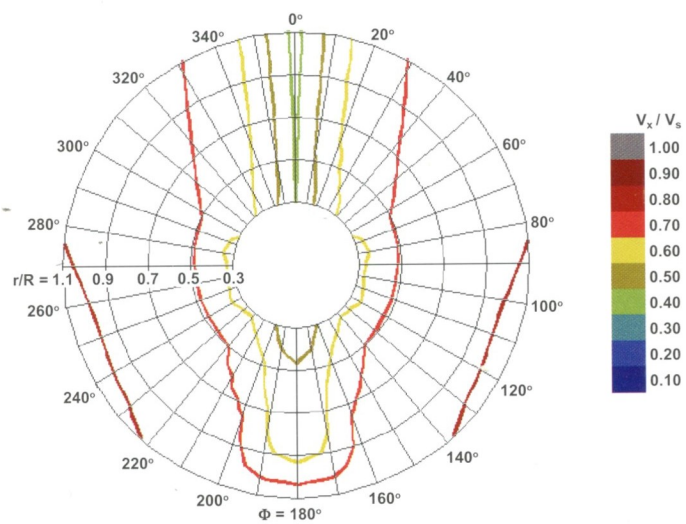

Fig.10. The axial component of the velocity field, obtained from the calculations of 4 m S-60 ship model, at V = 1.2 m/s

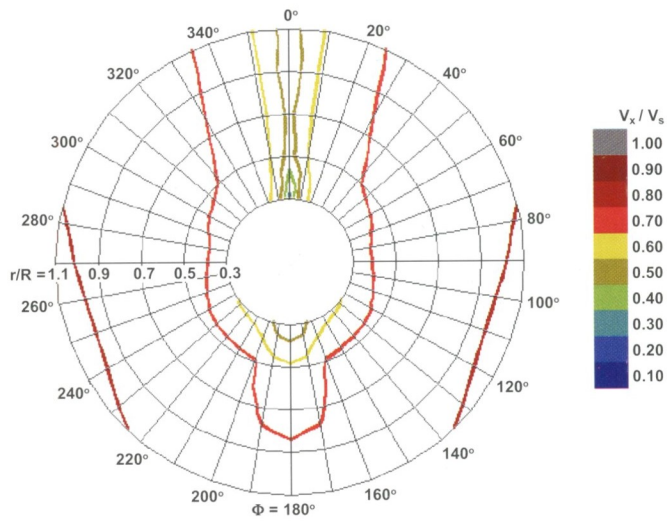

Fig.13. The axial component of the velocity field, calculated for 200 m S-60 ship model, at V = 8.485 m/s

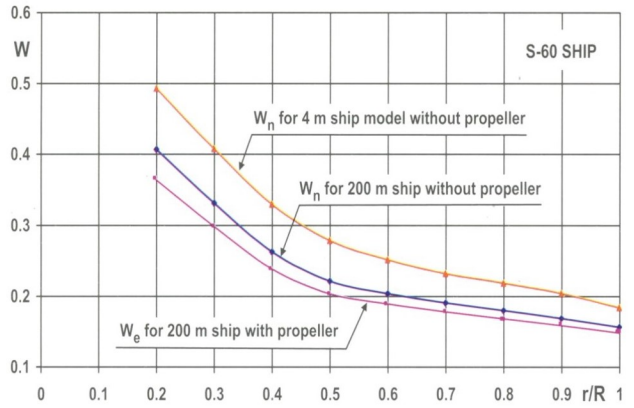

Fig.14. Radial distributions of the nominal wake fraction, W, for 4 m S-60 ship model (without a propeller), of the nominal wake fraction for 200 m S-60 ship (without a propeller) and the effective one for the same ship (with a propeller)

CALCULATION RESULTS FOR THE HULL OF THE CONTAINERSHIP

Data of the velocity field for the containership model of the block coefficient $C_B = 0.65$ were obtained from relevant measurements performed by Ship Hydrodynamics Department, Ship Design and Research Centre, Gdańsk. In Fig.15 the axial component of the velocity field, obtained from the measurements, is presented. A representation of the velocity field obtained from the calculations, is given in Fig.16. The differences are noticeable, but a character of the field is maintained.

The differences between the components of the effective velocity field for the ship of $L_{bp} = 200$ m and those of the nominal field for the model of $L_{bp} = 6.52$ m are presented in Fig.17. The differences take significant values.

The axial component of the effective velocity field for the 200 m ship, obtained after the modification of the model's velocity field (after accounting for the differences shown in Fig.17), are presented in Fig.18.

The same component of the effective velocity field, obtained from the calculations, is given in Fig.19. The observed changes are distinct because they take into account also the differences between the fields shown in Fig.15 and 16.

The changes in the velocity field result in the changes of the average values of the field. For instance, the radial distributions, presented in Fig.20, of the average value of the axial component of the field (wake fraction), for the nominal velocity field of the model and of the ship, as well as for the effective field of the ship, indicate that the influence of the scale effect and of propeller operation on the course of the distributions is significant.

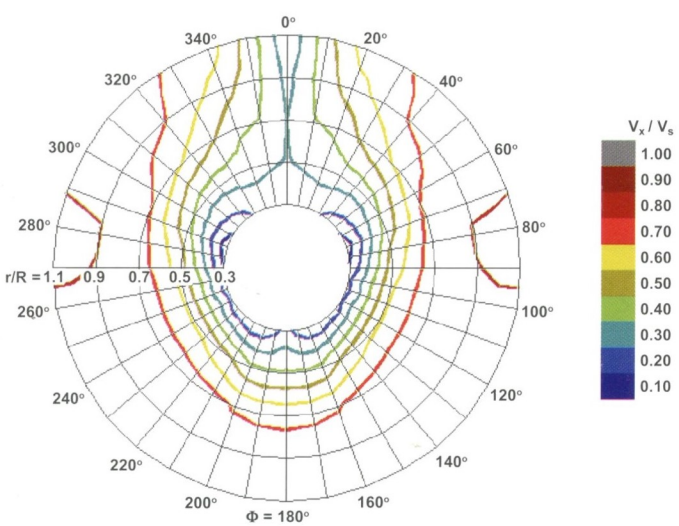

Fig.15. The axial component of the velocity field, obtained from the tests of 6.52 m containership model at V = 1.2 m/s

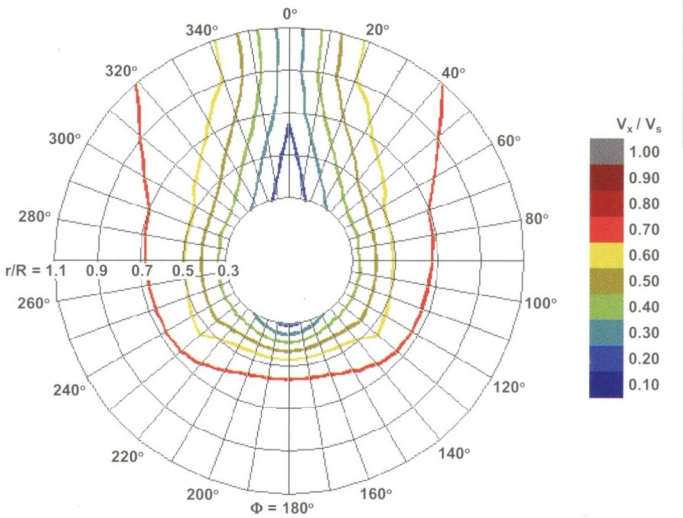

Fig.16. The axial component of the velocity field, obtained from the calculations for 6.52 m containership model at V = 1.2 m/s

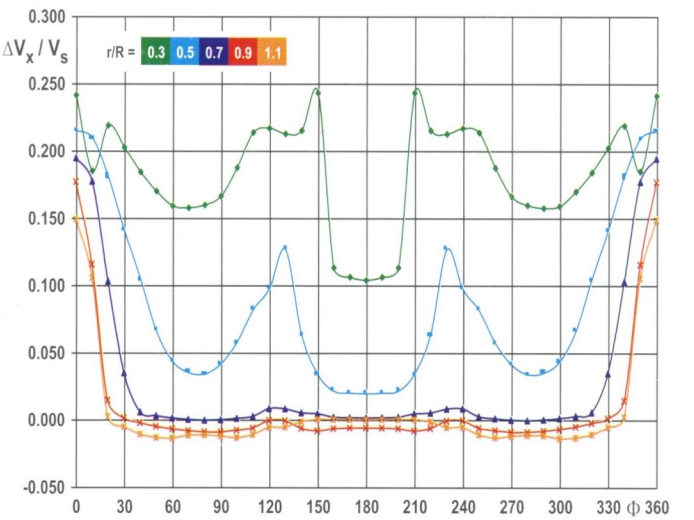

Fig.17. Differences, at different r/R values, between the axial component of the effective velocity field, V_x/V_s (Φ), for 200 m containership, and the axial component of the nominal velocity field for 6.52 m containership model

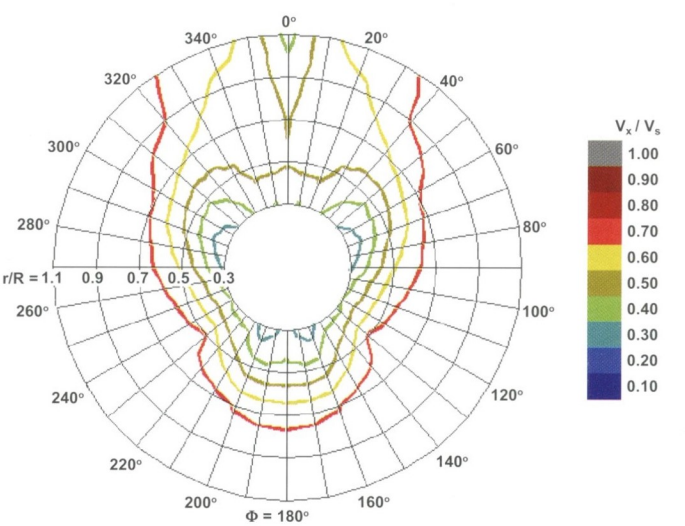

Fig.18. The axial component of the velocity field, for 200 m containership obtained from the tests of its 6.52 m model, at V = 1.2 m/s, modified with the use of the differences V_x/V_s (Φ) obtained from the calculations

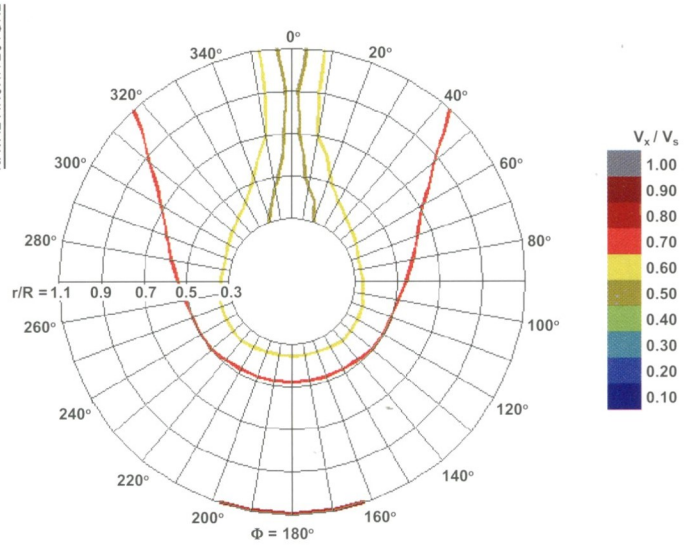

Fig.19. The axial component of the velocity field, obtained from the calculations for 200 m containership at V = 1.2 m/s

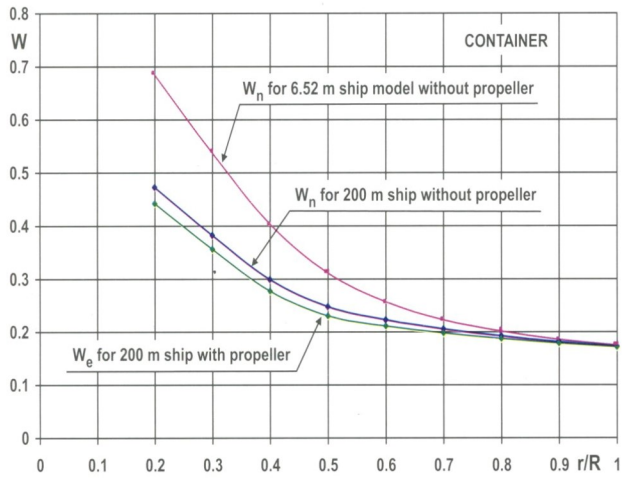

Fig.20. Radial distributions of the nominal wake fraction, W, for 6.52 m containership model (without a propeller), of the nominal wake fraction for 200 m containership (without a propeller) and the effective one for the same ship (with a propeller)

CALCULATIONS OF BEARING FORCES AND PRESSURES ON THE HULL

An imporant element of the screw propeller design process is the analysis of propeller performance in conditions of the full-scale ship velocity field. By applying the above presented results of tests and calculations it was possible to carry out the propeller performance analysis from the point of view of magnitude of the forces and moments transferred to the propeller shaft, as well as of the pressure pulses acting on the hull plating.

The calculations were performed with the use of UNCAVN software [3], a special, thoroughly verified computer program for analyzing performance of a screw propeller in the behind-the-hull velocity field. For each of the considered ships such calculations were carried out for two velocity fields :

- **the velocity field A** – i.e. that obtained from model tests, but the propeller working point (velocity and rotational speed) was so determined as to obtain values of the thrust and torque absorbed by the propeller, pertinent to those determined during propulsion tests
- **the velocity field B** – i.e. that modified according to the method proposed in this paper, under the same condition regarding thrust and torque values.

Results of the calculations for the ship of Series 60 and the velocity field A

Working and performance parameters of the screw propeller :
propeller diameter D = 5.3 m
speed V = 16.5 knots propeller revolutions n = 155 rpm
thrust T = 1100 kN torque Q = 1500 kNm

Tab.1. Components of forces (kN) and moments (kNm) acting on the propeller shaft (transformed into harmonics by using Fourier series)

	ΔF_x	ΔF_y	ΔF_z	ΔM_x	ΔM_y	ΔM_z
1st harmonic	213.7	43.8	43.5	217.7	191.1	140.8
2nd harmonic	12.3	5.2	5.3	11.7	36.8	35.0
3rd harmonic	8.6	3.0	2.0	8.1	15.1	8.2
4th harmonic	9.2	2.7	4.0	9.1	11.9	14.1

Tab.2. Amplitudes of the pressure acting on the hull plating (in kPa, transformed into harmonics by using Fourier series), calculated in 5 points over the propeller, having (x_{ph}, y_{ph}, z_{ph}) coordinates in the coordinate system connected with the propeller

x_{ph} [m]	0.0	0.0	0.0	0.5	- 0.5
y_{ph} [m]	0.0	0.745	- 0.745	0.0	0.0
z_{ph} [m]	5.3	5.65	5.65	5.37	5.23
1st harmonic	20.69	18.71	16.94	20.04	20.26
2nd harmonic	7.65	7.72	6.07	7.35	7.70
3rd harmonic	2.96	2.86	2.77	2.88	2.94
4th harmonic	1.58	1.59	1.37	1.54	1.59

Results of the calculations for the ship of Series 60 and the velocity field B

Tab.3. Components of forces (kN) and moments (kNm) acting on the propeller shaft (transformed into harmonics by using Fourier series)

	ΔF_x	ΔF_y	ΔF_z	ΔM_x	ΔM_y	ΔM_z
1st harmonic	100.8	23.6	18.6	102.1	116.4	78.0
2nd harmonic	32.4	1.2	2.0	33.3	6.8	4.6
3rd harmonic	17.1	1.6	0.8	17.3	8.9	2.0
4th harmonic	3.4	0.7	0.5	3.4	3.5	1.2

Tab.4. Amplitudes of the pressure acting on the hull plating (in kPa, transformed into harmonics by using Fourier series), calculated in 5 points over the propeller, having (x_{ph}, y_{ph}, z_{ph}) coordinates in the coordinate system connected with the propeller

x_{ph} [m]	0.0	0.0	0.0	0.5	- 0.5
y_{ph} [m]	0.0	0.745	- 0.745	0.0	0.0
z_{ph} [m]	5.3	5.65	5.65	5.37	5.23
1st harmonic	6.67	6.11	5.09	6.56	6.28
2nd harmonic	3.00	2.86	2.28	2.83	3.00
3rd harmonic	1.20	1.10	0.94	1.13	1.20
4th harmonic	0.43	0.39	0.40	0.42	0.44

Results of the calculations for the containership and the velocity field A

Working and performance parameters of the screw propeller :
propeller diameter D = 7.53 m
speed V = 21 knots propeller revolutions n = 105 rpm
thrust T = 2330 kN torque Q = 3030 kNm

Tab.5. Components of forces (kN) and moments (kNm) acting on the propeller shaft (transformed into harmonics by using Fourier series)

	ΔF_x	ΔF_y	ΔF_z	ΔM_x	ΔM_y	ΔM_z
1st harmonic	172.0	46.8	24.1	239.3	368.0	219.1
2nd harmonic	15.3	10.3	4.8	17.0	55.0	45.5
3rd harmonic	14.2	6.1	3.7	19.0	38.7	23.8
4th harmonic	12.5	3.2	1.7	17.0	22.2	9.0

Tab.6. Amplitudes of the pressure acting on the hull plating (in kPa, transformed into harmonics by using Fourier series), calculated in 5 points over the propeller, having (x_{ph}, y_{ph}, z_{ph}) coordinates in the coordinate system connected with the propeller

x_{ph} [m]	0.0	0.0	0.0	0.7	- 0.7
y_{ph} [m]	0.0	0.622	- 0.622	0.0	0.0
z_{ph} [m]	6.1	6.14	6.14	6.24	5.96
1st harmonic	8.54	8.58	8.220	8.47	8.03
2nd harmonic	8.37	8.19	8.00	8.05	8.19
3rd harmonic	5.14	5.04	4.89	4.93	5.03
4th harmonic	0.95	0.80	0.98	0.87	0.92

Results of the calculations for the containership and the velocity field B

Tab.7. Components of forces (kN) and moments (kNm) acting on the propeller shaft (transformed into harmonics by using Fourier series)

	ΔF_X	ΔF_Y	ΔF_Z	ΔM_X	ΔM_Y	ΔM_Z
1st harmonic	202.0	32.9	18.8	272.1	212.2	99.0
2nd harmonic	65.8	3.7	3.9	91.8	14.3	24.8
3rd harmonic	39.2	2.0	1.2	54.5	16.6	11.1
4th harmonic	9.5	1.1	1.3	12.8	8.3	12.8

Tab.8. Amplitudes of the pressure acting on the hull plating (in kPa, transformed into harmonics by using Fourier series), calculated in 5 points over the propeller, having (x_{ph}, y_{ph}, z_{ph}) coordinates in the coordinate system connected with the propeller

x_{ph} [m]	0.0	0.0	0.0	0.7	- 0.7
y_{ph} [m]	0.0	0.622	- 0.622	0.0	0.0
z_{ph} [m]	6.1	6.14	6.14	6.24	5.96
1st harmonic	3.66	3.79	3.23	3.21	4.06
2nd harmonic	3.09	2.97	2.91	2.90	3.05
3rd harmonic	2.26	2.22	2.10	2.19	2.15
4th harmonic	1.23	1.20	1.15	1.18	1.17

ANALYSIS OF THE RESULTS OBTAINED FOR BEARING FORCES AND PRESSURE PULSES ON THE HULL

The above presented results demonstrate how important is the influence of the modification of the model's velocity field on that of the full-scale ship for calculations of the bearing forces and presssure pulses on the hull.

For the two considered hull forms, the observed changes of values of the pressure pulses on the hull, were the greatest. For the modified velocity fields, distinctly more favourable results are obtained. This confirms the commonly accepted rule that the calculations of the pressure pulses on the hull, carried out on the basis of the model's field, give conservative results, i.e. on the safe side.

Smaller changes can be noticed in the case of the bearing forces, however they are not directed unambiguously. For instance, for the containership the model's field is more favourable than the modified one. It means that the application of the modified field to calculations of the bearing forces not always gives safe-side results as it is usually assumed in the case of the pressure pulses.

Nowadays more and more ships of the propeller power over 50 thou kW have entered service. Their problems concerning vibration of the hull and propulsion systems, are commonly known. In such cases comprehensive knowledge of the velocity field for the full-scale ship, already in the design phase, could help avoiding any bitter surprise during ship's delivery.

FINAL REMARKS

- The presented method of predicting the velocity field behind the full-scale ship hull has been currently tested during routine propulsion prognoses carried out by the Model Basin, simultaneously with a method based on ITTC recommendations and guidelines.
- The programs of PANSHIP-2 computer software are permanently under refinement. Its aim has been clearly defined and its final value would depend on results obtained from confrontation of its results with service experience of the real ships.

Appraised by Henryk Jarzyna, Prof.,D.Sc.

NOMENCLATURE

C_B - block coefficient [-]
F_n - Froude number $Fn = V / \sqrt{gL}$ [-]
g - acceleration of gravity [m/s²]
L - water line length [m]
L_{bp} - hull length beetwen perpendiculars [m]
r,Φ - coordinates in polar coordinate system connected with the propeller [m, grad]
R - propeller radius [m]
V - speed [knots, m/s]
V_r - radial component of the velocity filed
V_s - ship speed
V_t - tangential (circumferrential) component of the velocity filed
V_x - axial component of the velocity filed
W_e - effective wake fraction
W_n - nominal wake fraction
x_{ph}, y_{ph}, z_{ph} - coordinates of points on the hull in coordinate system connected with the propeller [m]
ΔF_x, ΔF_y, ΔF_z - harmonic amplitudes of components of forces acting on the propeller shaft [kN]
ΔM_x, ΔM_y, ΔM_z - harmonic amplitudes of components of moments acting on the propeller shaft [kNm]
$\Delta V_x / V_S$, $\Delta V_t / V_S$, $\Delta V_r / V_S$ - differences of components of velocity field related to the ship speed [-]
ITTC - International Towing Tank Conference
RANS - Reynolds Average Navier-Stokes

BIBLIOGRAPHY

1. Toda Y., Stern F., Tanaka I., Patel V.C.: *M-Flow Measurements in the Boundary Layer and Wake of a Series 60 C_B = 0.6 Model Ship With and Without Propeller.* Journal of Ship Research, Vol. 34, No. 4, December 1990
2. Bugalski T., Koronowicz T., Szantyr J., Waberska G.: *A Method for Calculation of Flow Around the Hull of a Ship Moving in Calm Water with Constant Velocity.* Marine Technology Transactions, No. 5, Gdańsk, 1994
3. Szantyr J.: *A Method for Analysis of Cavitating Marine Propeller in Non-Uniform Flow.* International Shipbuilding Progress, Vol. 41, No. 427, September 1994
4. Bugalski T., Grabowska K., Koronowicz T., Tuszkowska T.: *The Influence of Propeller Operation on the Pressure Field on the Hull and Around It.* Proceedings of XII Conference on Hydromechanics In Ship Design HYDRONAV'97. Szklarska Poręba, 17-19 September 1997
5. Koronowicz T., Kwapisz L., Wacławczyk T.: *The Velocity Field Prognosis Behind a Ship Hull in Full Scale*, Proceedings of Third International Shipbuilding Conference : ISC'2002. St. Petersburg, Russia

Conference

West–Pomeranian Regional Group

The Regional Group of Section on Exploitation Foundations, Machine Building Committee, Polish Academy of Sciences, acting in West-Pomeranian region of Poland, held, on 7 November 2002 , its next scientific meeting devoted to two papers :

- *On possible predicton of changes of exhaust gas emission from marine low-speed diesel engines with a view of selection of their operational characteristics* – by T. Borkowski
- *A test stand for investigations of oil separation process of sea waters* – by J. Listewnik, A. Wiewióra, and P. Treichel.

Their authors have been employees of the Institute of Technical Operation of Ship Power Plants, Mechanical Faculty, Maritime University of Szczecin, which organized the meeting.

After presentation of and discussion on the papers the laboratory test stand described in the second paper, was demonstrated to the meeting participants.